Available online at www.sciencedirect.com

SciVerse ScienceDirect

Ceramics International 38 (2012) 1887–1895

CERAMICS INTERNATIONAL

www.elsevier.com/locate/ceramint

Tribological behaviour of semisolid–semisolid compocast Al–Si matrix composites reinforced with TiB_2 coated B_4C particulates

Ali Mazahery, Mohsen Ostad Shabani *

Materials and Energy Research Center (MERC), Tehran, Iran

Received 23 August 2011; received in revised form 5 October 2011; accepted 6 October 2011
Available online 12 October 2011

Abstract

The purpose of this paper is to provide a deeper understanding of the wear behavior of the sol–gel coated B_4C particulate reinforced A356 matrix composites. A typical microstructure of the composite consists of relatively large primary phase globules which are surrounded by B_4C particles. In fact the globules themselves are B_4C particles free and consequently the sample is not homogeneous on a scale smaller than the globule size. The wear sliding test disclosed that the wear rate of the coated B_4C reinforced composites is less than that of the unreinforced alloy and decreases with increasing volume fraction of B_4C particulates. As the hardness of the composites is higher, this reduces the cutting efficiency of the abrasives and consequently the abrasion wear loss. Once the particles fracture or loosen from the matrix alloy, they can be removed easily from the matrix, contributing to the material loss. Two kinds of debris present irregular-shaped flake, which has withstood a large of plastic deformation and then pull off from the surface. During the sliding wear, Iron is transferred to the surface of the composites from the steel counterface forming the iron-rich layer on the contact surfaces which increases with increasing the B_4C content and is substantially harder than the bulk material largely because it contains a fine mixture of Fe phase, Al and B_4C.

Keywords: B. Composites; Wear; B_4C

1. Introduction

Large amount of castings are made annually from Al–Si alloy. This alloy is one of the most popular alloys used for aerospace, automobile, marine and mining industries due to its low density high specific strength, good corrosion properties, high fluidity and good castability [1,2]. However, the low hardness and poor wear resistance of aluminum alloys limit their use in certain tribological applications. The addition of high modulus refractory particles to a ductile metal matrix produces a material whose mechanical and tribological properties are intermediate between the matrix alloy and ceramic reinforcement. The optimum properties of metal matrix composites (MMCs) and enhanced performance from these materials, however, depend on a judicious selection of the metallic matrix material, reinforcing phase and the processing technique/parameters. The commonly used metallic matrices include light metals such as aluminum, magnesium, titanium and their alloys. Aluminum Matrix Composites (AMCs) which account for 69% of the annual metal matrix composites production by mass, have a very low coefficient of thermal expansion and high specific strengths, wear resistance and heat resistance as compared to the conventional Al alloys [3,4].

One of the major driving forces for the technological development of aluminum-matrix composites reinforced with ceramic whiskers/fibers/particles is a result of the fact that these composites possess superior wear resistance and are hence potential candidate materials for a number of tribological applications [5,6]. The wear resistance of aluminum alloys is improved as a consequence of the incorporation of ceramic fibers or particles which act as the load bearing and abrasive member. The enhancement in tribological properties of AMCs has been effectively attainable by introducing the ceramic particles, such as SiC, B_4C, Al_2O_3, TiC and AlN. There are excellent reviews on the tribology of aluminum-matrix composites [3,5–8]. It is reported that the wear resistance of the composite was found to be considerably higher than that of the matrix alloy and increased with increasing particle content.

* Corresponding author. Tel.: +98 912 563 6709; fax: +98 261 6201888.
E-mail address: vahid_ostadshabany@yahoo.com (M.O. Shabani).

0272-8842/$36.00
doi:10.1016/j.ceramint.2011.10.016

However, there have been discrepancies among the reported results. These discrepancies may come from the large number of variables which can affect wear behavior, including the applied load, test geometry, test duration, materials properties, and environmental factors, such as temperature, humidity, etc.

Researchers reported that the addition of hard ceramic particles as a reinforcement to aluminum alloys supported and protected the aluminum matrix from wear and minimized sever surface shear strain that was associated with the unreinforced alloys. The matrix structure also influences the wear and friction behaviors of MMCs, so that the processing route and/or heat treatment conditions can enhance the wear resistance of these materials via their effects on the matrix microstructure, distribution of particles, porosity content, particle matrix bonding and mechanical properties [9–13].

In the present study, Boron carbide powder was chosen as reinforcement because of its higher hardness than the conventional and routinely used reinforcement such as SiC, Al_2O_3. Further its density is very close to Al alloy matrix. This specific property comes along with other attractive properties such as high impact and wear resistance, low density, high melting point, and excellent resistance to chemical agents as well as high capability for neutron absorption [14].

According to the type of reinforcement, the fabrication techniques can vary considerably. These techniques include squeeze casting, liquid metal infiltration, spray decomposition and powder metallurgy [15]. In order to overcome some of the drawbacks associated with the conventional stir casting techniques, semisolid agitation processes which are often referred to as compocasting can be employed. The benefits include reduced solidification shrinkage, lower tendency for hot tearing, suppression of segregation, settling or agglomeration and faster process cycles.

These advantages are accompanied with lack of superheat (lower operating temperatures) as well as a lower latent heat which results in a longer die life together with a reduced chemical attack of the reinforcement by alloy, also a globular, non-dendritic structure of the solid phase which then explains the thixotropic behavior of the material [16,17].

The wettability of B_4C particles represents a very important issue which is poor at temperatures near the melting point of aluminum (660 °C) [18]. In this study, attention was paid to the fact that B_4C powders coated with some of Ti-compounds might have reasonable wettability with aluminum [19–22]. The coated reinforcement is added to a semisolid matrix alloy and the mixture is agitated vigorously. The presence of the primary solid phase in the viscous semisolid imposes an abrasive action on clumps of undispersed reinforcement in the slurry which assists the incorporation of the ceramic particles. The solidified metallic particles also prevent the non-metallics from settling, floating or agglomerating, resulting in a more homogeneous particle distribution as compared with a fully molten alloy. Finally, the microstructure and wear properties of the composites have been experimentally investigated.

2. Experimental procedure

In this study, a commercial casting-grade aluminum alloy (A356) {(wt.%): 7.5 Si, 0.38 Mg, 0.02 Zn, 0.001 Cu, 0.106 Fe, and Al (balance)} was employed as the matrix material. This alloy has been selected because of its good fluidity as well as the presence of silicon and magnesium. Since the silicon content of A356 alloy is sufficiently high, it can be maintained in the liquid state at typical casting temperatures for certain periods of time without giving rise to the extensive formation of Al_4C_3. The liquidus temperature of this alloy is 615 °C and its relatively large semisolid interval makes it suitable for semisolid processing. The presence of Mg in this alloy is thought to improve the wetting of the reinforcement by the liquid alloy.

The conventional reinforcement materials for A356 are SiC and Al_2O_3. Due to the higher cost of B_4C powder relative to SiC and Al_2O_3, limited research has been conducted on B_4C reinforced MMCs. In this study, specific quantities of B_4C with average particle sizes of 1, 10, 21, 33, 42 and 55 μm were added to the matrix alloy.

The chemical composition of B_4C is represented in Table 1. The grain size of B_4C particles was analyzed using a Malvern laser size analyzer. Attempts were made to coat the B_4C powders with TiB_2 via a sol–gel process and incorporate them into the A356 alloy by a mechanical stirrer. This treatment helps the incorporation of the particles while reducing undesired interfacial reactions. Indeed in a preliminary experiment, uncoated B_4C particles were mostly rejected from the melt.

Titanium tetraisopropoxide (TTIP) or $Ti[OCH(CH_3)_2]_4$ with the purity of 97% was selected as a sol–gel precursor and diluted with ethanol (C_2H_5OH). For coating of the titanium oxide, boron carbide powders were dispersed in ethanol, stirred well, and then TTIP and distilled water were added to the stirred suspension. The processing was conducted at room temperature at a solution pH of 7. Distilled water for hydrolysis was previously diluted by ethanol to inhibit the rapid hydrolysis of TTIP. Approximately, 0.1 M concentration of Titanium tetraisopropoxide (TTIP) solution was prepared and added to 1 g of B_4C. The amount of water was adjusted to 4 times that of TTIP. The solution was then aged for 105 min at room temperature, with constant, gentle stirring. When TTIP is used as the precursor, TiO_2 can be produced by hydrolysis and heat treatment. The reactions occur as follows:

$$Ti[OCH(CH_3)_2]_4 + 4H_2O = Ti(OH)_4 + 4C_3H_7OH \quad (1)$$

$$Ti(OH)_4 = TiO_2 + 2H_2O \quad (2)$$

Titanium oxide does not support good wettability for aluminum. However, it is converted to TiB_2 when heated with boron

Table 1
Chemical composition of B_4C.

Total boron	Total carbon	Total iron	Total B + C
77.5%	21.5%	0.2%	98%

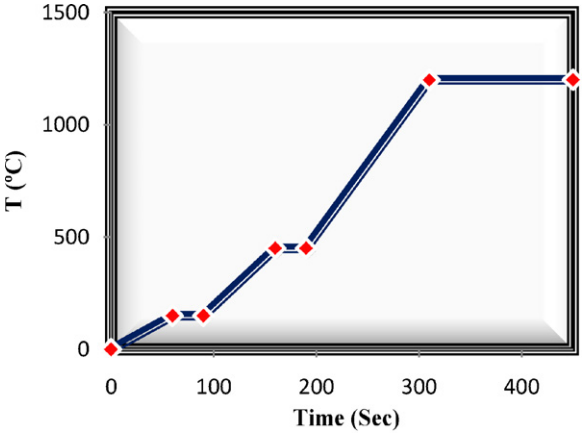

Fig. 1. Heat treatment cycle on B_4C powders after sol–gel process.

carbide. As the temperature increases or the pressure decreases, the reactions become more favorable.

$$B_4C + 2TiO_2 + 3C\,(\text{graphite}) = 2TiB_2 + 4CO \quad (3)$$

The powders were heat treated in a graphite crucible and under Argon atmosphere.

After the sol–gel process, the powders were paper-filtered and dried at 140 °C. When needed, sucrose was introduced in water solution. Fig. 1 shows the heat treatment cycle that was implemented to eliminate the adsorbed water and to achieve a TiB_2 coating. Fig. 2 represents X-ray diffraction (XRD) analysis of the coated powders.

A relatively simple experimental set-up was used in this experiment which is depicted in Fig. 3. The main part allows temperatures of up to 1000 °C to be reached. This is surrounded by a 50 mm thick layer of kaowool insulator to minimize heat loss. Inside the heater band is a graphite crucible of 2 kg capacity for holding the materials, which has a lid. Batches of the matrix alloy were melted in the graphite crucible using an electrical resistance-heated furnace. The furnace is controlled using a J-type thermocouple located inside the gas chamber. The temperature of the alloy was first raised to about 700 °C and then stirred at 800 rpm using an impeller fabricated from graphite and driven by a variable ac motor. The temperature of

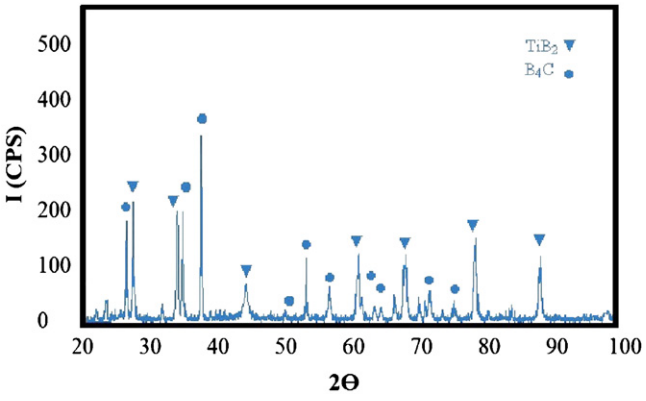

Fig. 2. XRD pattern of the coated B_4C powders.

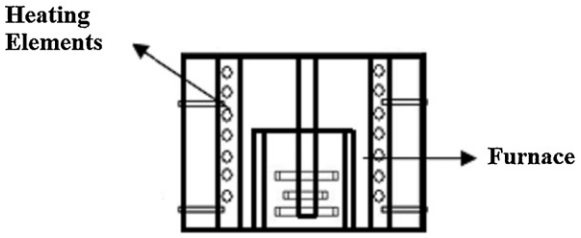

Fig. 3. Schematic diagram of the experimental set-up.

the furnace was gradually lowered until the melt reached a temperature in the liquid–solid range (i.e. 590 °C) while stirring was continued. Then the stirrer was positioned just below the surface of the slurry and the coated particles were added uniformly at a rate of 50 g/min over a time period of approximately 1–3 min. At the conclusion of charging the slurry was allowed to mix in the semisolid state isothermally for another 30 min while the stirrer was positioned near the bottom of the crucible. For manufacturing of the composites, 2.5, 5, 7.5, 10, 12.5 and 15 vol.% B_4C particles were used. A continuous purge of nitrogen gas is used inside and outside of the crucible to minimize the oxidation of molten aluminum and graphite parts. Magnesium additive in powder form was also used as a wetting agent. The addition of 1 wt.% magnesium to the melt promote wetting by reducing the surface tension of the melt, decreasing the solid–liquid interfacial energy of the melt, or inducing wettability by chemical reaction. The squeeze casting was obtained by pouring composite slurry into preheated permanent die and punch which was allowed to solidify under squeeze pressure of 80 MPa for duration of 5 min. High temperature graphite powder was used in the die to facilitate removal of cast blanks from the die after cooling. The pressure applied during solidification in the squeeze casting technique results in excellent feeding during solidification shrinkage. For the purpose of comparison, unreinforced A356 alloy was also cast following the procedures which were identical to those for the composite samples.

The experimental density of the composites was obtained by the Archimedian method of weighing small pieces cut from the composite cylinder first in air and then in water, while the theoretical density was calculated using the mixture rule according to the weight fraction of the particles. The porosities of the produced composites were evaluated from the difference between the expected and the observed density of each sample. The microstructures of the produced ingots were examined using a scanning electron microscope to determine the distribution of the B_4C particles.

The quantitative assessment of the B_4C particle distribution within composite samples was performed by considering the distribution factor (DF) defined as:

$$DF = \frac{S.D.}{A_f}$$

In which A_f is the mean value of the area fraction of the B_4C and S.D. is its standard deviation. The volume fraction of B_4C

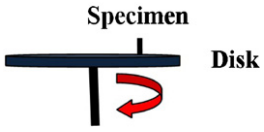

Fig. 4. Schematic diagram of the abrasion wear test.

particles was measured via an image analyzer system attached to an optical microscope.

Specimens for the wear tests were solution treated at 540 °C for 4 h, quenched into warm water (40 °C) and then peak aged to T6 condition (155 °C for 9 h).

Dry sliding wear tests were performed using a pin-on-disc type wear apparatus. The slider disc was case hardened steel with 63 HRC to a depth of 3 mm. Fig. 4 shows Schematic diagram of the abrasion wear test. Test specimens were cut and shaped in the form of pins having 6 mm in diameter and 25 mm in height. Before the abrasion tests, each specimen was polished to 0.5 μm. Wear tests were carried out at room temperature (21 °C, relative humidity 55%) with water as lubricant. The test parameters were: normal load of 10 N and total sliding distance of 2000 m. The weight losses were calculated from the differences in weight of the specimens measured before and after the tests to the nearest 0.1 mg using an analytical balance. A separate specimen was used to measure the weight loss for each sliding distance. The wear test was interrupted at regular intervals and the incremental weight loss of the sample was recorded. After each increment and before weighing, the disc and the pin were cleaned in an ultrasonic bath with acetone and hot wind dried below 100 °C.

3. Results and discussion

The XRD pattern of the B_4C reinforced composites is displayed in Fig. 5. It can be seen that B_4C and aluminum are present and various reaction products are formed in the system, including the deleterious Al_4C_3 phase. The maximum solubility of boron and carbon in aluminum is relatively low, thus these two elements rapidly dissolute and saturate the melt. Subsequently, other products nucleate on impurity seeds or at the B_4C surface from the supersaturated melt. Growth continues via a classical dissolution–precipitation mechanism. In all the samples, the peaks for the TiB_2 phase and the low amount of reaction products were noted. Thus, most of initial boron carbide and aluminum remain unreacted, indicating phases are conserved for desirable applications [14].

The uniformity in distribution of particles within the sample is a microstructural feature which determines the in-service properties of particulate AMCs. A non-homogeneous particle distribution in cast composites arises as a consequence of sedimentation (or flotation), agglomeration and segregation. The subject of particle distribution in particulate MMCs has been studied by several investigators either qualitatively or quantitatively. The macroscopic particle segregation due to gravity (settling) has also been studied both experimentally and theoretically, the latter of which generally involves the correlation of particle settling rate within the composite slurry with the Stocks' low [23–27].

The microstructures of the composites were examined using an optical microscope to determine the distribution of the B_4C particles and presence of porosity. It is reported that the high viscosity of the semisolid alloy slurry imparts shear force over the agglomerates and aids in better separation of the dispersoids. The volume fraction of B_4C particles was measured by means of an image analyzer system attached to the optical microscope. A typical microstructure of an Al/B_4C composite is presented in Fig. 6 which consists of relatively large primary phase globules, surrounded by B_4C particles. The distribution of the B_4C particles within the matrix alloy was characterized by a distribution factor (DF). Fig. 7 shows the gradual improvement in the uniformity of the B_4C particle distribution (as reflected by decreased DF) for the composites when the particle content increased. These results can be attributed to the restricted movement of particles within the melt during solidification as a consequence of the increased effective viscosity of the slurry and the less pronounced coarsening effects resulting in a finer matrix microstructure which in turn causes a more uniform ceramic particle

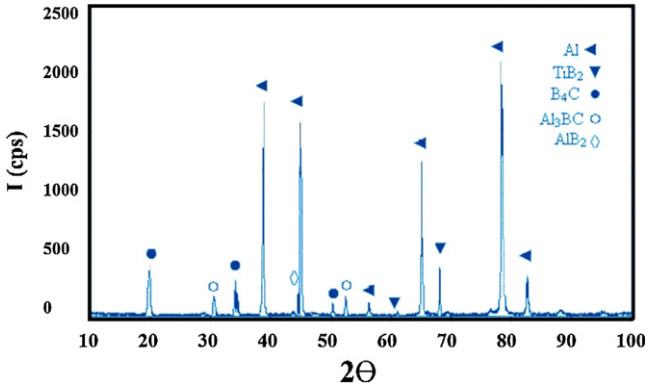

Fig. 5. XRD pattern of the composite with 10 vol.% coated B_4C.

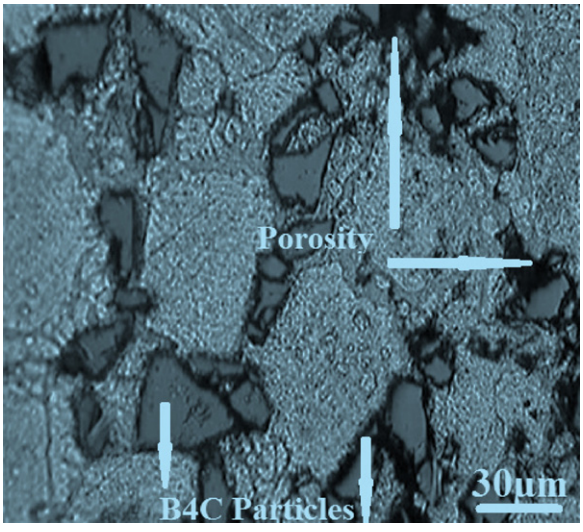

Fig. 6. Typical optical microscope micrograph of the composites.

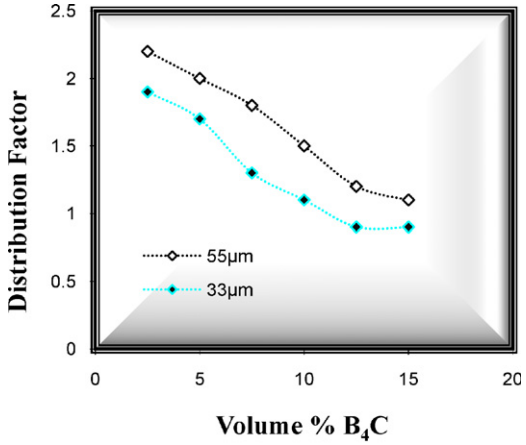

Fig. 7. The distribution factor versus the B_4C particles content.

distribution. Fig. 7 shows that for composites containing a fixed B_4C content, there is an improvement in the particles distribution corresponding to a decrease in particle size. In compocast composite, due to the presence of some primary solid phase at the instant of casting, the extent of particle pushing is reduced. Thus, when finer particles are used, the more refined microstructure is influential to obtain more uniform particle distribution. In fact, a careful control on temperature, shear rate and processing conditions is required to produce defect-free castings with fine spheroidised microstructure which in turn may exhibit a more uniform particle distribution.

A sedimentation experiment was conducted on the composites containing 12.5 vol.% of 33 μm sized particles. Fig. 8 shows the B_4C concentration as a function of the distance from the bottom of the mould (D), representing an even macroscopic particle distribution. The semisolid slurry showed no particle settling. In fact, the relatively high viscosity of the semi molten alloy did not allow the movement of reinforcement particles due to gravity.

The microstructures of the coated composites were also examined by Scanning Electron Microscope in order to determine the distribution of the B_4C particles and presence of porosity. Typical SEM micrographs of the compocast B_4C reinforced Al alloy composites are shown in Fig. 9. It is observed that fabrication of these composites via compocasting technique lead to reasonably uniform distribution of particles in the matrix and minimum clustering or agglomeration of the reinforcing phase.

One of the major problems associated with the cast AMCs is porosity formation which has been studied by several authors [28,29]. In the processing of these composites a considerable portion of the slurry is already solidified at the instant of casting, so that porosity arising from the solidification shrinkage is reduced. However, due to a relatively high viscosity, the semisolid composite slurry cannot vent air as a fully molten alloy. Also the lower latent heat and a high solid fraction in the semisolid metal provide quicker melt solidification. This effect in turn reduces the available time for gas escape and thereby increases the porosity level. The

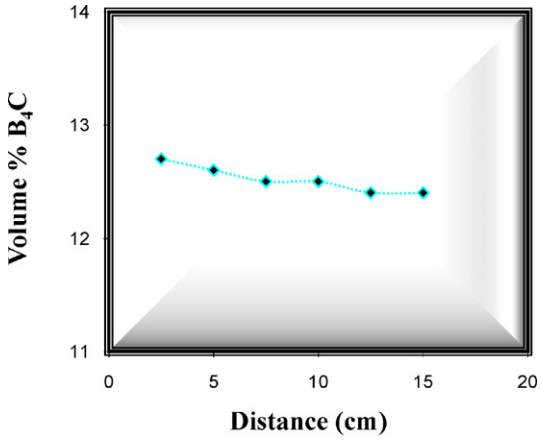

Fig. 8. The B_4C concentration versus the distance from the bottom of the mould (D).

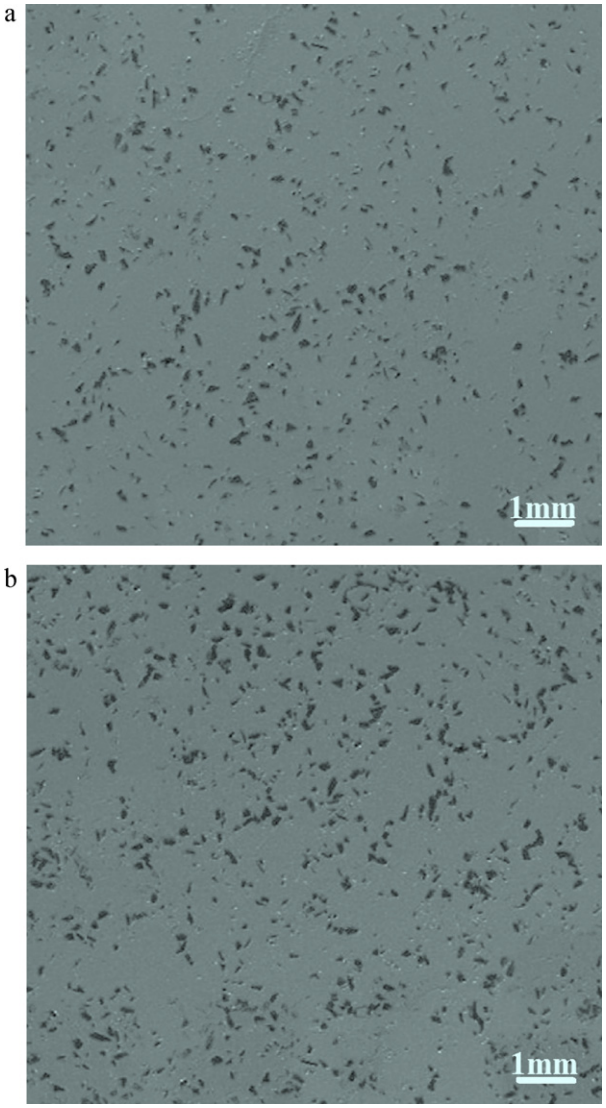

Fig. 9. Typical SEM micrographs of the composites with (a) 7.5 vol.% coated B_4C, (b) 12.5 vol.% coated B_4C.

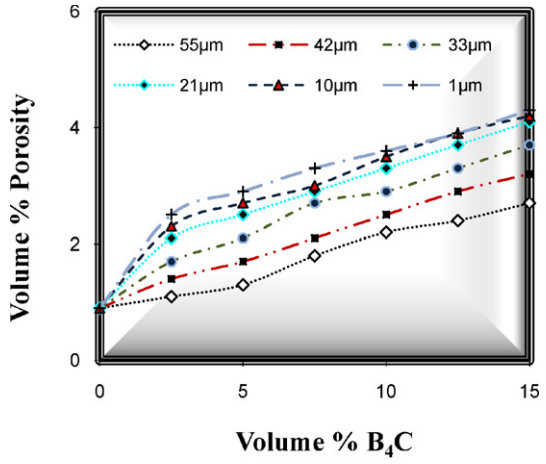

Fig. 10. The variation of porosity content versus volume percent of B_4C.

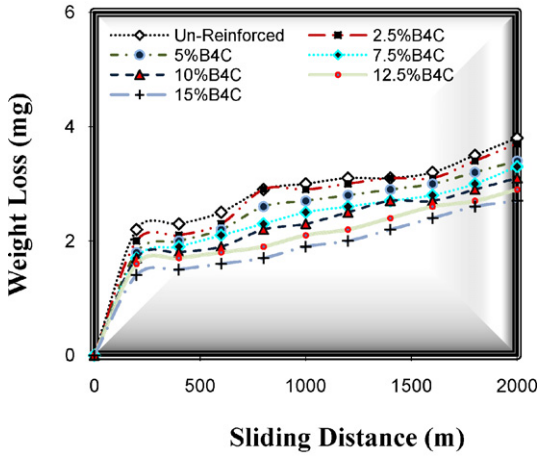

Fig. 11. Typical variations of wear loss as a function of sliding distance (10 μm).

variation of porosity with the B_4C content is shown in Fig. 10. It can be seen that for composites containing a fixed size of B_4C particles, there is an increase in the vol.% porosity corresponding to an increase in the vol.% B_4C incorporated. The porosity is normal, because of the increasing effective viscosity of suspension and the increase in surface area in contact with air caused by increasing the particle content. Fig. 10 shows that for a fixed content of B_4C particles, the porosity of both composite samples decreases with increasing size of B_4C particles. This trend is also reported by the early works [30–32] and is attributed to increasing surface gas layers surrounding particles and porosity associated with the particle clusters. Decreasing the particle size for a fixed volume fraction of particles increases the probability for B_4C particle clustering. The air trapped in the cluster of particles as well as the hindered liquid metal flow inside them in turn contribute to the formation of porosity. In this study, the pressure immediately applied after the casting, has reduced the porosity in the composites, and improved the bonding force between the Al alloy and B_4C particles.

The tribological behavior of particulate reinforced AMCs has been generally found to be a function of the applied load as well as the reinforcement volume fraction, particle size, and the shape and nature of the reinforcing phase. The matrix structure also influences the wear and friction behaviors of MMCs, so that the processing route and/or heat treatment conditions can enhance the wear resistance of these materials via their effects on the matrix microstructure, distribution of particles, porosity content, particle matrix bonding and mechanical properties [3,5–13].

The typical variation of the composites weight loss with sliding distance is shown in Fig. 11. It is clear that the weight losses of the composites are less than that of unreinforced alloy and has a declining trend with increasing the particles volume fraction. The hard particles resist against destruction action of abrasive and protect the surface, so with increasing its content, the wear resistance enhances. This result is consistent with the rule that in general, materials with higher hardness have better wear and abrasive resistance.

Fig. 12 shows the changes in the friction coefficient (μ) with sliding distance. The coefficient of friction is a composite function of the extent to which the energy is dissipated in the pin and the disc. It can be seen that the friction coefficient of the composite specimen is lower than that of the unreinforced alloy. In the composite, the reinforcement particles support the load, so as to lessen the touch area between the pin and counter disc surface, decrease the friction coefficient and can prevent the scratch and cut from the surface [7]. This is probably the main reason for the observed enhancement in wear resistance of the composite. It is reported in literature that good dispersion and better interface of the particle in matrix leads to a lower value of coefficient of friction. In addition, the higher formation of Fe rich layer on the worn surface may contribute to lower the coefficient of friction (by acting as a lubricant) [8,11]. Iron, and possibly other alloying elements, from the steel counterface are transferred to the surface of the composites during sliding wear. The formed layer on the worn surfaces of the pins is stable and compacted layer called mechanically mixed layer (MML). MML is substantially harder than the bulk material largely because it contains a fine mixture of Fe phase, Al and B_4C.

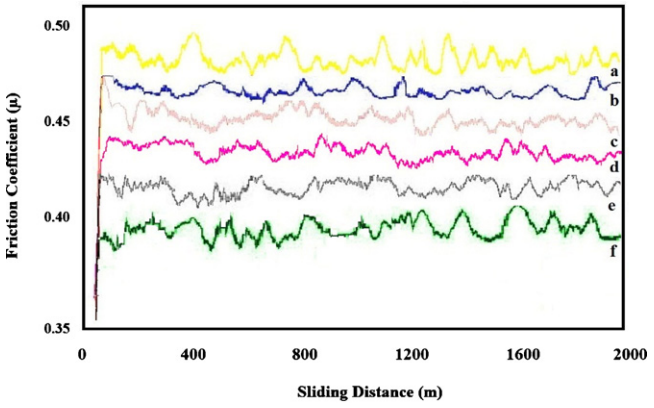

Fig. 12. Effect of sliding distance and particle sizes on friction coefficient (μ): (a) Unreinforced 2024 Al alloy; Composites with 7.5 vol.% B_4C (b) 1 μm, (c) 10 μm, (d) 21 μm, (e) 42 μm and (f) 55 μm.

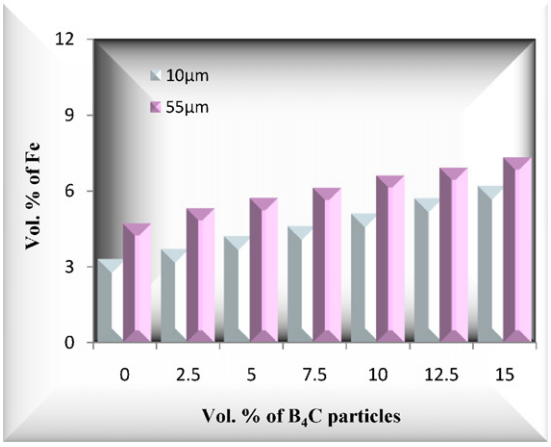

Fig. 13. Variations of the Fe content on the worn surface with B_4C content.

Fig. 13 shows the Fe content variation on the worn surface with B_4C content. It is observed that the formation of iron-rich layers on the contact surfaces increases with increasing the B_4C content. The source of iron in the layer is obviously the steel disc against which the pins have been slid during the wear test. It is very likely that during the initial stages of sliding, the B_4C particulates present in the composite pin plough into the steel disc and thus create a debris mostly containing iron. Iron may be present either as iron or as iron oxide. It is reported that iron might get oxidized during this process and oxide layers, in particular Fe_2O_3 layers generated during wear, act as solid lubricants and help to reduce the wear rates [33–36].

It can be noted that not only volume fraction of the B_4C particles, but also average size of them plays a significant role on wear behavior of composites. In Fig. 14 which also represents the variation of the composites weight loss with sliding distance, a transition from severe to mild wear is observed. This transition can be attributed to the formation of MML. It was reported in the previous research that when the applied load induces stresses that exceed the fracture strength of carbide particles, the particles fracture and largely lose their effectiveness as load bearing components. The shear strains are transmitted to the matrix alloy and wear proceeds by a subsurface delamination process. In this case, the lower ductility of Al–B_4C composites appears to control the wear rates rather than the hardness of particles, resulting in wear rates almost similar to those observed in Al alloys without B_4C reinforcement. On the other hand, when the nominal load induces stresses lower than the strength of particles the particles act as load bearing components. In this case, the B_4C particles remain intact during wear in order to support the applied load and act as effective abrasive elements. The particles protruding from the surface of the composite bear most of the wear load, and the surface hardness of the composite is mainly a result of the hardness of the particles [35,36].

Wear debris can be generated by microcutting, plastic deformation as well as material transfer from one surface to another [6]. Fig. 15 depicts the propagation of cracks and formation of wear debris which is loosely bound to the wear surface. As the hardness of the composites is higher, this reduces the cutting efficiency of the abrasives and consequently the abrasion wear loss. Once the particles fracture or loosen from the matrix alloy, they can be removed easily from the matrix, contributing to the material loss. Fig. 16 shows typical SEM micrographs of wear debris of the unreinforced and composite samples. Two kinds of debris present irregular-shaped flake, which has withstood a large of plastic deformation and then pull off from the surface. A typical flaky morphology of debris of the unreinforced alloy is shown in Fig. 16(a), indicating the process of delamination. Fig. 16(b) shows that the debris of the composites comprised of a mixture of the fine particles and small shiny metallic plate-like flakes. The shape and size of these loose wear debris denotes that a mild wear regime was dominant during its generation process.

In general, displacement of material at the edges of the wear grooves resulted in the liberation of sheet-like wear debris and adhesive wear could produce irregularly shaped debris. The process of delamination leads to flaky morphology of debris which involves the nucleation of subsurface cracks and their propagation parallel to the surface and finally generation of

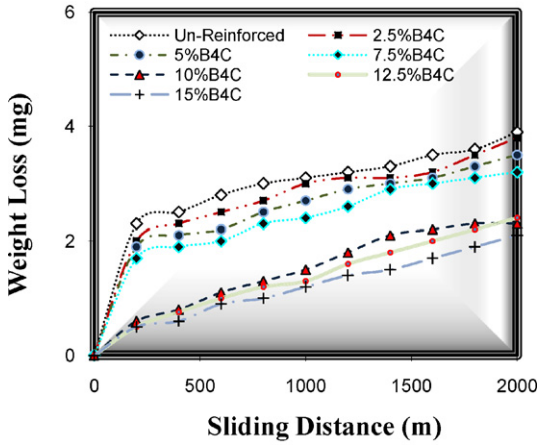

Fig. 14. Variations of wear loss as a function of sliding distance (55 µm).

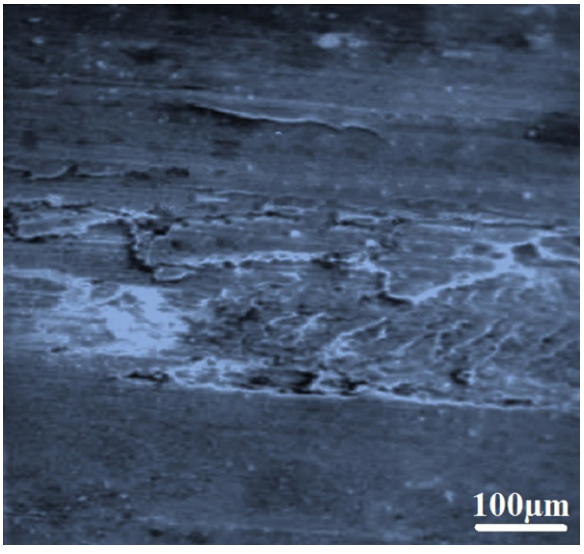

Fig. 15. The formation of wear debris on the worn surface.

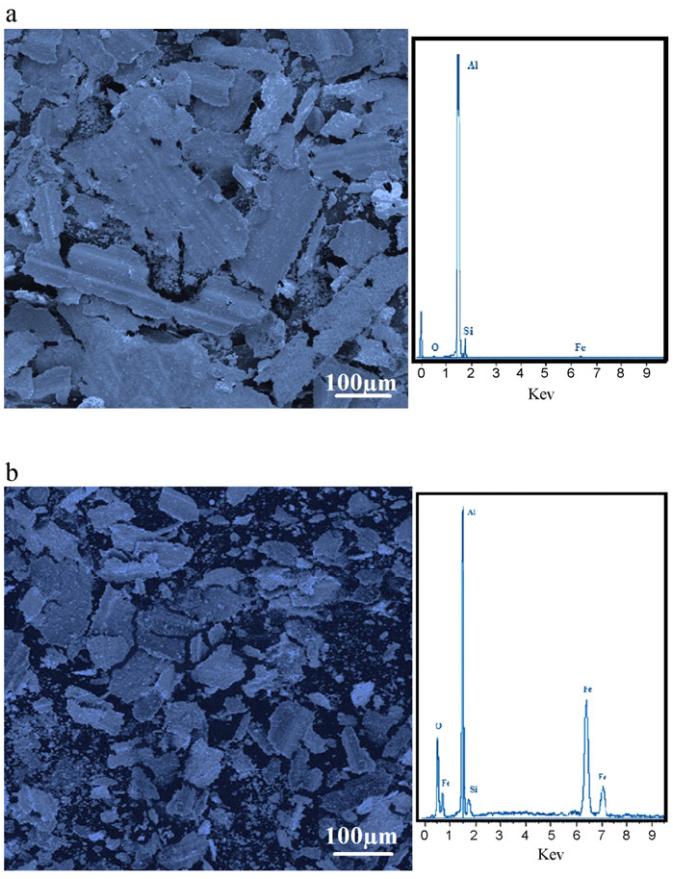

Fig. 16. SEM micrographs and EDS analyses of the wear debris: (a) Unreinforced A356 alloy, (b) A356–15% B_4C particles (44 μm).

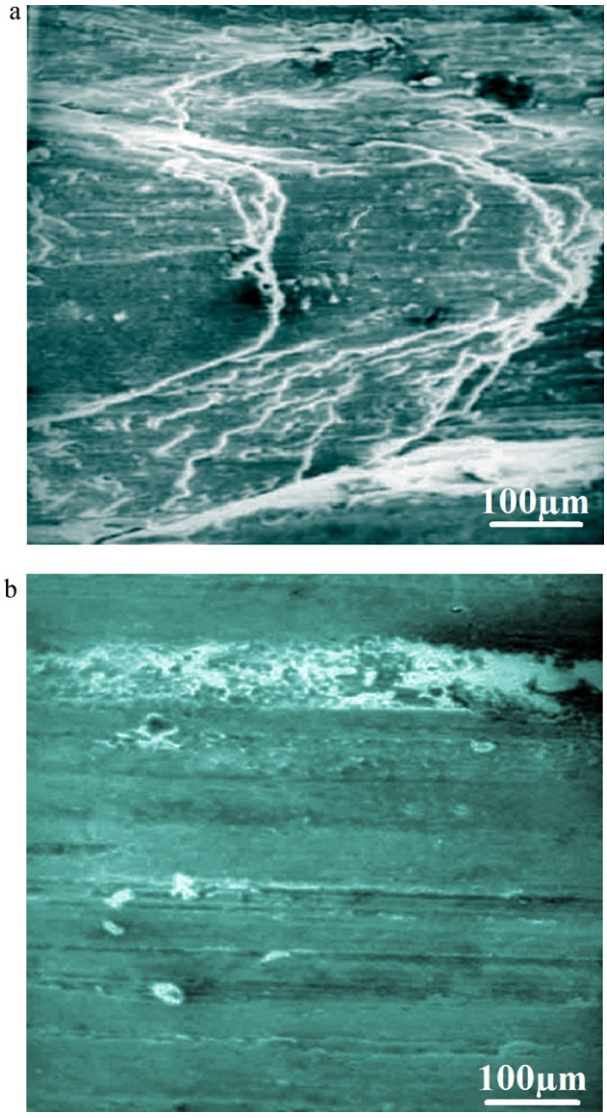

Fig. 17. SEM micrographs of worn surfaces: (a) Unreinforced A356 alloy, (b) Al–15% B_4C particles (42 μm).

wear debris [35]. It is interesting to be noted that during the wear process, the flaky shaped debris are formed essentially by the joining of longitudinal and the transverse cracks. Aluminum, oxygen and traces of iron were detected by EDS analysis. This observation confirms the presence of oxidized material which is the typical of an oxidative wear mechanism. The presence of oxidized material suggests the formation of an oxide tribolayer or MML. The transfer of material between the mating surfaces, the existence of fragments of oxide material and/or oxide layers and the mechanical mixture and compaction of these fragments on the surface promotes the formation of a MML. Delamination of the MML suggests the continuous destruction and formation of this layer of material on the wear track. Also, the previously discussed load-bearing action of the particles can help the accommodation of material and subsequent formation of MML.

The worn surface of the composite materials sliding against steel counterpart is evaluated in order to elucidate the wear mechanisms. Generally, the worn surfaces of all specimens were covered with grooves parallel to the sliding direction and some plastic deformations. These grooves are typical features associated with abrasive wear, in which hard asperities on the steel counterface or hard particles between the pin and disc, plough or cut into the pin causing wear by the removal of the material. Plastic deformation, material smearing, cavities and craters imply adhesive wear [35]. Fig. 17(a) shows a typical worn surface of the unreinforced alloy. The unreinforced A356 alloy is seized at loads lower than the applied load of 10 N and therefore the wear surface is characterized by the flow of materials along the sliding direction, generation of cavities due to delamination and tearing of surface. It is noted that the slider could penetrate and cut deeply into the surface and cause an extensive plastic deformation on the surface, resulting in a great amount of material loss. The worn surface of samples was characterized by plate like plastic flow and plastically deformed grooves along sliding direction, which were the consequence of abrasive action by hard asperities or particles. The wear surface of the composite with 15 vol.% B_4C at the applied load of 10 N is shown in Fig. 17(b). It indicates the formation of continuous wear grooves and patches of damaged regions. However, the degree of cracks formation on the wear surface is not much. Unlike the worn surface of the unreinforced alloy, the number of scratches by abrasives or hard asperities was small. Worn

surfaces of the composites were smoother with shallower grooves along the sliding direction. Therefore, it was reasonable that wear resistance of composites was higher than that of the unreinforced alloy.

4. Conclusion

In order to overcome some of the drawbacks associated with the conventional stir casting techniques, semisolid agitation process is employed to incorporate the TiB_2 coated B_4C powders into the aluminum matrix. XRD patterns show that most of initial boron carbide and aluminum remain unreacted, indicating phases are conserved for desirable applications. Analysis of particles distribution revealed a gradual improvement in the uniformity of the B_4C particles when the particle content increased. The wear resistance of the composite was found to be considerably higher than that of the matrix alloy and increased with increasing particle content. Based on the weight loss data, composites with 15 vol.% B_4C particles have the highest wear resistance among all the tested samples and unreinforced aluminum alloys give the lowest wear resistance. The friction coefficient of the composite specimen is seen to be lower than that of the unreinforced alloy. The results show that with an increase in the particle size, the wear weight losses of the composites are substantially reduced in comparison with the matrix alloy.

References

[1] E.A. Vieira, M. Ferrante, Prediction of rheological behaviour and segregation susceptibility of semi-solid aluminium–silicon alloys by a simple back extrusion test, Acta Mater. 53 (2005) 5379–5386.

[2] M.O. Shabani, A. Mazahery, Application of finite element method for simulation of mechanical properties in A356 alloy, Int. J. Appl. Math. Mech. 7 (2011) 89–97.

[3] P.N. Bindumadhavan, T.K. Chia, M. Chandrasekaran, H.K. Wah, L.N. Lam, O. Prabhakar, The mechanical response of Al–Si–Mg/SiCp composite: influence of porosity, Mater. Sci. Eng. A 315 (2001) 217–226.

[4] S. Nagarajan, B. Dutta, The effect of SiC particles on the size and morphology of eutectic silicon in cast A356/SiCp composites, Compos. Sci. Technol. 59 (1999) 897–902.

[5] M.O. Shabani, A. Mazahery, Prediction of wear properties in A356 matrix composite reinforced with B_4C particulates, Synth. Met. 161 (2011) 1226–1231.

[6] S. Chung, B.H. Hwang, A microstructural study of the wear behaviour of SiCp/Al composites, Tribol. Int. 27 (5) (1994) 307–314.

[7] S.C. Lim, M. Gupta, L. Ren, J.K.M. Kwok, The tribological properties of Al–Cu/SiCp metal-matrix composites fabricated using the rheocasting technique, J. Mater. Process. Technol. 89/90 (1999) 591–596.

[8] M. Roy, B. Venkataraman, V.V. Bhanuprasad, Y.R. Mahajan, G. Sundararajan, Correlation between the characteristics of the mechanically mixed layer and wear behaviour of aluminium, Al-7075 alloy and Al-MMCs, Metall. Trans. A 23 (1992) 2833–2846.

[9] S. Skolianos, T.Z. Kattamis, Tribological properties of SiC reinforced Al–4.5% Cu–1.5% Mg alloy composites, Mater. Sci. Eng. A 163 (1993) 107–113.

[10] M.K. Surappa, S.V. Prasad, P.K. Rohatgi, Wear and abrasion of cast Al-alumina particle composites, Wear 77 (1982) 295–302.

[11] P.N. Bindumadhavan, H.K. Wah, O. Prabhakar, Dual particle size (DSP) composites: effect on wear and mechanical properties of particulate metal matrix composites, Wear 248 (2001) 112–120.

[12] J.K.M. Kwok, S.C. Lim, High-speed tribological properties of some Al/SiCp composites: II. Wear mechanisms, Compos. Sci. Technol. 59 (1999) 55–65.

[13] S. Das, D.P. Mondal, G. Dixit, Correlation of abrasive wear with microstructure and mechanical properties of pressure die-cast aluminum hard-particle composite, Metall. Mater. Trans. A 32 (2001) 633–642.

[14] J.C. Viala, J. Bouix, G. Gonzalez, C. Esnouf, Chemical reactivity of aluminium with boron carbide, J. Mater. Sci. 32 (1997) 4559–4560.

[15] S.M.L. Nai, M. Gupta, Influence of stirring speed on the synthesis of Al/SiC based functionally gradient materials, Compos. Struct. 57 (2002) 227–233.

[16] C.J. Quaak, W.H. Kool, Properties of semisolid aluminium matrix composites, Mater. Sci. Eng. A 188 (1994) 277–282.

[17] J. Hashim, L. Looney, M.S.J. Hashmi, Particle distribution in cast metal matrix composites. Part I, J. Mater. Process. Technol. 123 (2002) 251–257.

[18] W.R. Blumenthal, G.T. Gray, T.N. Claytor, Response of aluminium-infiltrated boron carbide cermets to shock wave loading, J. Mater. Sci. 29 (1994) 4567.

[19] A.J. Pyzik, I.A. Aksay, M. Sarikaya, Processing and microstructural characterization of B_4C–AI cermets, Mater. Sci. Res. 21 (1986) 45.

[20] A.J. Pyzik, I.A. Aksay, Processing of ceramic and metal matrix composites, in: Proceedings of the International Symposium on Advances in Processing of Ceramic and Metal Matrix Composites, New York, NY, (1989), p. 269.

[21] A.J. Pyzik, D.R. Beaman, Al–B–C phase development and effects on mechanical properties of B_4C/Al-derived composites, J. Am. Ceram. Soc. 78 (1995) 305.

[22] S.K. Rhee, Wetting of AlN and TiC by liquid Ag and liquid Cu, J. Am. Ceram. Soc. 53 (1970) 386.

[23] L.V. Vugt, L. Froyen, Gravity and temperature effects on particle distribution in Al–Si/SiCp composites, J. Mater. Process. Technol. 104 (2000) 133–144.

[24] G.A. Irons, K. Owusu-Boahen, Settling and clustering of silicon carbide particles in aluminium metal matrix composites, Metall. Mater. Trans. B 26 (1995) 980–981.

[25] S. Gowri, F.H. Samuel, Effect of cooling rate on the solidification behavior of Al–7 Pct Si–SiCp metal-matrix composites, Metall. Trans. A 23 (1992) 3369–3376.

[26] M. Gupta, L. Lu, S.E. Ang, Effect of microstructural features on the aging behaviour of Al–Cu/SiC metal matrix composites processed using casting and rheocasting routes, J. Mater. Sci. 32 (1997) 1261–1267.

[27] P.A. Karnezis, G. Durrant, B. Cantor, Characterization of reinforcement distribution in cast Al-alloy/SiC composites, Mater. Charact. 40 (1998) 97–109.

[28] U. Cocen, K. Onel, The production of Al–Si alloy–SiC composites via compocasting: some microstructural aspects, Mater. Sci. Eng. A 221 (1996) 187–191.

[29] M.O. Shabani, A. Mazahery, Modeling of the wear behavior in A356–B_4C composites, J. Mater. Sci. 46 (2011) 6700–6708.

[30] A.M. Samuel, A. Gotmare, F.H. Samuel, Effect of solidification rate and metal feedability on porosity and SiC/Al_2O_3 particle distribution in an Al–Si–Mg(359) alloy, Compos. Sci. Technol. 53 (1995) 301–315.

[31] R. Chen, G. Zhang, Casting defects and properties of cast A356 aluminium alloy reinforced with SiC particles, Compos. Sci. Technol. 47 (1994) 277–282.

[32] M. Gupta, M.O. Lai, M.S. Boon, N.S. Herng, Regarding the SiC particles size associated microstructural characteristics on the aging behaviour of Al–4.5 Cu metallic matrix, Mater. Res. Bull. 33 (2) (1998) 199–209.

[33] K.C. Ludema, A review of scuffing and running-in of lubricated surfaces, with asperities and oxides in perspective, Wear 100 (1984) 315–331.

[34] S.C. Lim, M.F. Ashby, Quantitative wear maps as a visualization of wear mechanism transitions in ceramic materials, Acta Metall. 35 (1987) 1–24.

[35] A. Mazahery, M.O. Shabani, The accuracy of various training algorithms in tribological behavior modeling of A356–B_4C composites, Russ. Metall. (Metally) (2011) 699–707.

[36] K. Razavizadeh, T.S. Tyre, Oxidative wear of aluminium alloys, Wear 79 (1982) 325–333.